Available online at www.sciencedirect.com
ScienceDirect
Journal of Nuclear Materials 367–370 (2007) 995–1002
journal of nuclear materials
www.elsevier.com/locate/jnucmat

Effects of neutron irradiation on the properties of functional materials for fusion applications: Role of hydrogen in radiation effects on oxide ceramics

Tatsuo Shikama [a,*], Bun Tsuchiya [a], Eric R. Hodgson [b]

[a] *Institute for Materials Research, Tohoku University, 2-1-1Katahira, Aobaku, Sendai 980-8577, Japan*
[b] *EURATOM/CIEMAT, Madrid 28040, Spain*

Abstract

Effects of hydrogen (proton) in the electrical conductivity of ceramics were studied, with protonic conductive perovskite-oxides. Large electrical conductivity was observed at elevated temperatures under fission reactor irradiation, which could be explained by the contribution of protonic conduction. At elevated temperatures, existence of high concentration hydrogen (proton) will increase the ionic conductivity. Reduction of ions constituting the oxides was observed in electron irradiation as well as 14 MeV neutron irradiation at room temperature, which will result in radiation induced phase changes. The results imply that role of hydrogen in radiation effects in oxide ceramics is important, which may evoke technological problems in fusion machines.

1. Introduction

It is well recognized that radiation effects in functional materials will be among the most important issues to be understood for the development of nuclear fusion reactors. Under the circumstances where allocation of research resources are limited to the concerned research fields, international collaborations have been strongly promoted through activities such as the ITER–EDA (Engineering Design Activity) [1,2], and the International Tokamak Physics Activity (ITPA) [3]. Several critical issues have been studied and the results have been reviewed and reported in appropriate international conferences and symposiums [4–7]. Main issues are summarized as follows:

1. Radiation induced degradation of electrical insulating ability of ceramics (radiation induced electrical conductivity (RIC) and radiation induced electrical degradation (RIED)) [8–10].
2. Performance of fused silica (SiO_2) core optical fibers and other optical materials under fusion relevant irradiation conditions [6,11,12].
3. Radiation induced electro-motive-force in mineral insulating cables (MI-cables) and other metals/ceramics systems [13–16].
4. Performance of components whose major constituents are functional materials, such as a

* Corresponding author. Tel.: +81 22 215 2060; fax: +81 22 215 2061.
E-mail address: shikama@imr.tohoku.ac.jp (T. Shikama).

0022-3115/$ - see front matter © 2007 Elsevier B.V. All rights reserved.
doi:10.1016/j.jnucmat.2007.03.231

bolometer (electrically conductive metallic meander and electrically and thermally insulating substrate) [17], a magnetic sensor [18,19] and a JxB sensor [20] (windings of electrically conductive wires and electrical insulators).

The ITER–EDA and the ITPA also pointed out other important issues to be studied, as follows:

(a) Radiation effects on sensor materials for plasma diagnostics, such as radiation flux, optical density and thermal flux detectors, as well as temperature detectors.
(b) Radiation effects on piezoelectric elements for remote position-adjusting systems and on Peltier elements for local heat removals [1,20].
(c) Life evaluation of sheathed thermocouples under fusion relevant irradiation conditions.
(d) Radiation effects in charge coupled devices (CCD) for remote visual inspection.

Among the issues summarized above, electrically degrading behavior of ceramic insulators have attracted strong concerns, especially in the early stage of the ITER–EDA because it will introduce serious technological problems in designing fusion machines, where many electrical components will be exposed to intense radiation environments [1,2]. Extensive studies resulted in the conclusion that the degradation of electrical insulation will not cause serious problems in design of the ITER, for electronic-conductive ceramic insulators such as alumina (Al_2O_3) [9,10].

However, modification of electrical properties of ceramics by radiation effects is still attracting strong attention. Electrical charges will be transported in ceramics not only by electrons but also by electron–holes, ions, and protons. Especially in nuclear fusion environments, electrical conductivity by proton migration (protonic conduction) will play an important role, as the supply of hydrogen isotopes is sufficient and working temperature for ceramics will in general be high. Also, reduction of oxide ceramics by radiation effects is another topic which is attracting interest. Some observed degradation of electrical insulation may be attributed to formation of electrically conductive phases such as gamma-alumina (Al_2O_4) and aluminum colloids in alpha-alumina (Al_2O_3) [8].

In the present paper, radiation effects on the electrical conductivity of perovskite-type oxides will be reviewed, emphasizing radiation effects on the transport behavior of hydrogen and on reducing behavior of oxide ceramics [21–23]. Some perovskite-type oxides are known to have large protonic conductivity and the electrical charge state of elements comprising them can easily be studied by spectroscopic techniques.

2. Experimental procedures

Three kinds of perovskite-type oxides, ytterbium doped strontium–cerium oxide ($SrCeO_3$), ($SrCe_{0.95}Yb_{0.05}O_{3-\delta}$), yttrium doped barium–cerium oxide ($BaCeO_3$), ($BaCe_{0.9}Y_{0.1}O_{3-d}$), and indium doped calcium–zirconium oxide ($CaZrO_3$), ($CaZr_{0.9}In_{0.1}O_{3-d}$), were irradiated in the Japan Materials Testing Reactor (JMTR) in the Oarai Research Establishment of Japan Atomic Energy Research Institute (JAERI; now Japan Atomic Energy Agency (JAEA)). Their electrical conductivity was measured in situ during the reactor irradiation. The fast ($E > 1.0$ MeV) and the thermal ($E < 0.683$ eV) neutron fluxes were in the range of 1×10^{16}–6×10^{17} and 1×10^{17}–1.6×10^{18} n/m^2 s, respectively. The associated gamma-ray dose rates were in the range 0.1–2.0 kGy/s. Subcapsules, each of which contained one specimen, were accommodated in an instrumented rig with a partially circulating purified helium atmosphere at 2 atmospheres-pressure. After the reactor reached its steady-state operation mode at 50 MW, the temperature was controlled by electric heaters as well as by changing a helium gas pressure between the subcapsule and the irradiation rig.

The measurement setup for the electrical conductivity was reported elsewhere [21,24]. The guard-ring configuration was adopted, with the guard ring connected to the ground potential through a wall of the subcapsule holding the specimen. Thin zirconium films were deposited on both sides of a plate-like specimen as electrodes and two platinum wires were connected to the two zirconium electrodes, working as a cathode and an anode. The guard ring electrode was connected to a stainless-steel subcapsule wall through a thick copper specimen holder to circumvent a leakage electrical current from coming into a current-measuring-side electrode. To study the protonic conductivity, 10 keV proton ions were implanted into the anode side zirconium film and oxygen ions into the cathode side.

A similar irradiation was carried out in the fast neutronic source (FNS) of the Tokai Research

Establishment in the JAEA to study effects of 14 MeV neutrons from the deuterium/tritium nuclear reaction, in an ambient atmosphere with the neutron fluxes in the range of 1×10^{9}–3×10^{12} n/m^2 s, where the accompanying gamma-ray dose rate is very small [22]. To study spectroscopic behavior, 1.8–2.0 MeV electron-irradiation was carried out in vacuum, in the Center of Investigation for Energy and Environmental Technologies (EURATOM/CIEMAT), measuring the in situ electrical conductivity, optical absorption and luminescence during the irradiation [23].

After the irradiations, conventional metallurgical examinations were carried out, including X-ray photo spectroscopy (XPS), scanning electron microscopy (SEM) with energy dispersion spectroscopy (EDS) for the specimens irradiated by the electrons and the 14 MeV neutrons.

3. Experimental results and discussions

3.1. Electrical conductivity without hydrogen injection into the zirconium electrode

The base electrical conductivity of the present perovskite-type oxides is relatively high and the radiation induced (enhanced) electrical conductivity was marginal when the hydrogen (proton) did not participate in the electrical conduction. Fig. 1 shows the electrical conductivity of $SrCe_{0.95}Yb_{0.05}O_{3-d}$, increased by 8×10^{-9} S/m from the base electrical conductivity under the 1.8 MeV electron irradiation [23] with a 10 Gy/s dose rate, which is within the range of scatter of accumulated data of the radiation induced electrical conductivity (RIC) of several ceramic insulators shown in Fig. 2 [25]. In the meantime, the base electrical conductivity decreased from 4.6×10^{-8} S/m to about 5×10^{-10} S/m after the 2.85 MGy irradiation. A similar decrease of the base electrical conductivity was observed in the 14 MeV neutron irradiations at 293 and 373 K. The observed decrease of the base electrical conductivity is thought to be related to a radiation induced reduction, namely change of a charge state of ions in the oxides. In the case of $SrCe_{0.95}Yb_{0.05}O_{3-d}$, Ce^{4+}, this may being reduced to Ce^{3+}, which will be discussed in Section 3.3 [23].

With decrease of the base electrical conductivity from 2×10^{-8} S/m to about $(2–5)\times10^{-10}$ S/m, a radiation induced (enhanced) electrical conductivity of about 2×10^{-9} S/m surfaced even in 14 MeV neutron irradiation at 293 K [22], after the irradiation up to about 2×10^{18} n/m^2. The electronic excitation dose rate was estimated to be in the range of 10^{-2} Gy/s and the observed increase of the electrical conductivity was higher than the accumulated RIC data as shown in Fig. 2. Hydrogen atoms picked up from the atmospheric environment may play a role in the observed radiation induced (enhanced) electrical conductivity. Effects of hydrogen will be discussed in Section 3.2.

At 1.9 kGy/s irradiation at 473 K during the JMTR irradiation, the observed electrical conductivity of $SrCe_{0.95}Yb_{0.05}O_{3-d}$ was about 1×10^{-5} S/m at the beginning of irradiation and 1×10^{-6} S/m after 2.8×10^{23} n/m^2 fast neutron fluence. The electrical conductivity of 1.2×10^{-6} at the beginning of the irradiation and 6×10^{-7} S/m at 3.6×10^{23} n/m^2 fast neutron fluence, at 2 kGy/s were observed for $BaCe_{0.9}Y_{0.1}O_{3-d}$ at about 520 K, and 8×10^{-7} S/m at 230 Gy/s for $CaZr_{0.9}In_{0.1}O_{3-d}$ at about

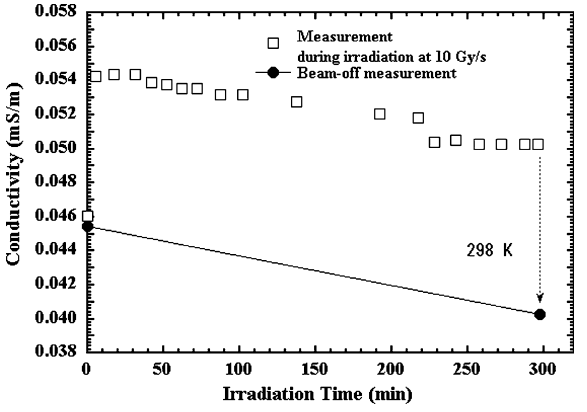

Fig. 1. Electrical conductivity of $SrCe_{0.95}Yb_{0.05}O_{3-d}$ under 1.8 MeV electron irradiation at 297 K.

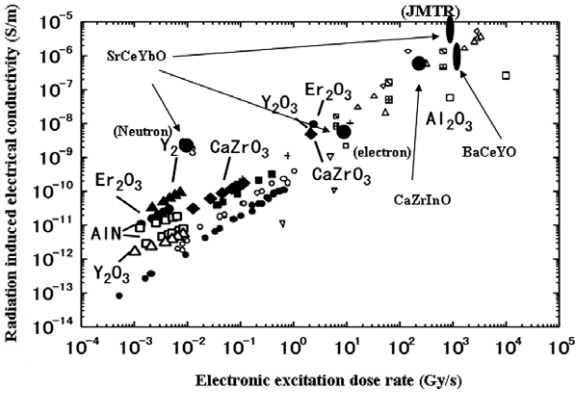

Fig. 2. Electrical conductivity under the irradiation (RIC data compiled by T. Tanaka [26]).

420 K, all of which are also within the scatter of accumulated RIC data [25] shown in Fig. 2. However, it should be pointed out that the temperature dependence of the electrical conductivity was large even under the 2 kGy/s irradiation as will be described below, which is strongly suggesting that the observed electrical conductivity was not dominated by the electronic conduction of conventional RIC. Decrease of the electrical conductivity was also observed in the JMTR irradiation in the course of irradiation as described above.

At about room temperature, the electrical conduction especially without irradiation will be dominated mainly by the electrons (or the electron holes), in these oxides [26]. The observed decrease of the base electrical conductivity at about room temperature under the electron and 14 MeV neutron irradiations will correspond to suppression of the electronic (or hole) conductivity by radiation induced modification of microstructures of the oxides. Above about 420–550 K, the protonic conduction will play a significant role in these oxides [26,27]. Even when the oxides are not intentionally doped with hydrogen, the concentration of residual hydrogen trapped in the oxides will be substantial and will contribute to the electrical conduction. The observed decrease of the electrical conduction in the course of the JMTR irradiation at elevated temperature may correspond to suppression of protonic conduction, for example, by a decrease of the residual hydrogen concentration or by a decrease of the mobility of hydrogen with increase of the trap sites introduced by radiation. The observed radiation induced (enhanced) electrical conductivity, under 14 MeV neutron irradiation at room temperature, after the decrease of the base electrical conductivity, may be explained by the contribution of the proton conduction, enhanced by the 14 MeV neutron irradiation even at room temperature.

3.2. Effect of hydrogen implantation into anode zirconium electrode and temperature dependence of electrical conductivity

The electrical conductivities of $BaCe_{0.9}Y_{0.1}O_{3-d}$ with one hydrogen implanted in its anode zirconium film and another without hydrogen implantation (hereafter denoted as a specimen with hydrogen and a specimen without hydrogen) are shown in Fig. 3 as a function of the electronic excitation dose rate at the startup of JMTR. It is clearly shown that the specimen with hydrogen had larger electrical

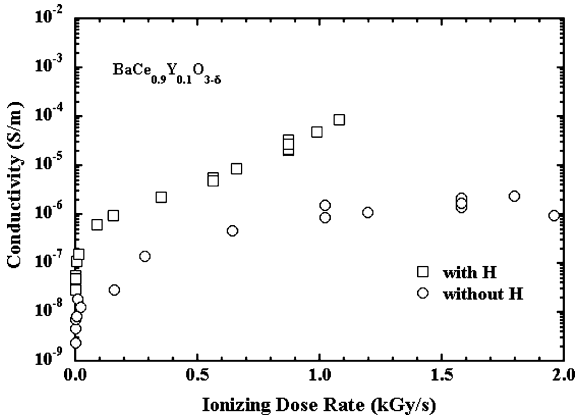

Fig. 3. Electrical conductivity of $SrCe_{0.95}Yb_{0.05}O_{3-d}$ at JMTR startup.

conductivity than that without hydrogen. Two other oxides, $SrCe_{0.95}Yb_{0.05}O_{3-d}$ and $CaZr_{0.9}$-$In_{0.1}O_{3-d}$ showed similar results. The results clearly showed that the hydrogen implantation into an anode increased the electrical conductivity. The observed increase of electrical conductivity, both in the specimens with hydrogen and without hydrogen, with the increase of the reactor power (thus the increase of the neutron flux and the electronic excitation dose rate) does not directly correspond to the increase of the normal radiation induced electrical conductivity (RIC). In normal RIC, the electronic conductivity is dominant and the RIC has very weak temperature dependence, in the present case, the electrical conductivity observed during the JMTR irradiation had a large temperature dependence.

Fig. 4 shows the temperature dependence of the electrical conductivity of $BaCe_{0.9}Y_{0.1}O_{3-d}$ [28] or non-irradiation conditions (a bench top experiment), the electrical conductivity is composed of two mechanisms, one having a lower apparent activation energy of about 0.2 eV (mechanism 1) in the temperature range below 480 K, and the other having a higher apparent activation energy of about 0.7–0.8 eV (mechanism 2) [27,29]. The hydrogen implantation into the anode did not substantially alter the electrical conductivity by mechanism 1 but increased the electrical conductivity by mechanism 2 by about the two orders of magnitude. During the JMTR irradiation, temperature dependence of the electrical conductivity below about 400 K could not be measured due to a large nuclear heating rate. However, the electrical conductivity by mechanism 2 could be clearly observed, and was enhanced by the irradiation. Without the hydrogen

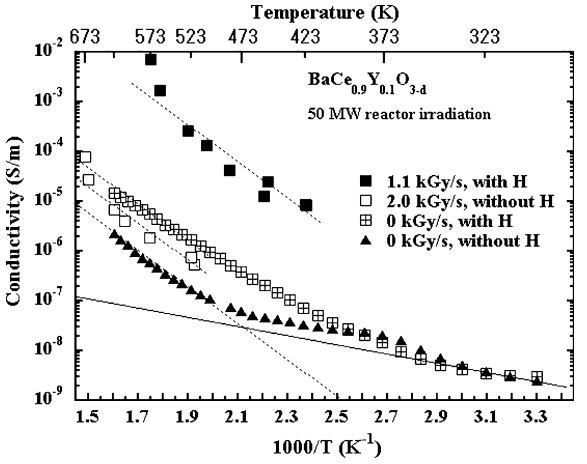

Fig. 4. Temperature dependence of electrical conductivity of $BaCe_{0.9}Y_{0.1}O_{3-d}$, without irradiation and under JMTR irradiation [28].

implantation into the anode, the increase of the electrical conductivity of mechanism 2 by 2 kGy/s irradiation was about 7 times. In the meantime, measurements with the hydrogen implanted anode showed an observed increase of electrical conductivity by the 1.1 kGy/s irradiation was more than two orders of magnitude. Under the JMTR irradiation, a further increase of the electrical conductivity (by mechanism 3) above that by mechanism 2 was observed at higher temperatures, namely, above 623 K for the specimen without hydrogen and above 523 K for the specimen with hydrogen. This increase of the electrical conductivity at higher temperatures was not observed in the bench top unirradiated experiments as can be seen in Fig. 4.

Mechanism 1 with the apparent activation energy of about 0.2 eV is interpreted to correspond to the electron-conduction or the electron–hole conduction. Without hydrogen, the electrical conduction will be dominated by mechanism 1 below 450 K, thus, the RIC, which has very weak temperature dependence, may be observable below 450 K. A quasi-linear dependence of the observed electrical conductivity on the electronic excitation dose rate below 450 K in the specimen without hydrogen, shown in Fig. 3 (data following dotted line) supports this hypothesis.

Mechanism 2 with an apparent activation energy of about 0.7–0.8 eV corresponds to the protonic-conduction and mechanism 3 is due to the ionic conduction of ions constituting the oxide. Decrease of the electrical conductivity at about 293 K in the electron irradiation and the 14 MeV neutron irradiation and below 473 K in the JMTR irradiation is due to the decrease of electrical conductivity by mechanism 1, resulting from microstructural modification of the oxide caused by radiation. The decrease of electrical conductivity by mechanism 1 is assumed to relate to a change of charge state of ions composing the oxide, which will be described below.

The electrical conductivity by mechanism 2 was enhanced substantially under irradiation. As the apparent activation energy was not affected by the irradiation, the concentration of a charge carrier, namely a proton, must be increased by the irradiation, assuming that mechanism 2 corresponds to the protonic conduction. Thus, the irradiation will enhance ionization of hydrogen and penetration of protons into the oxide. Increase of the electrical conductivity by mechanism 3 strongly suggests that mobility of ions composing the oxide is also increased by the irradiation. The appearance of mechanism 3 at lower temperatures in the specimen with hydrogen implies that the existence of protons will enhance the increase of ion mobility by the irradiation.

Enhancement of the ion migrations by the irradiation was also implied by the surface morphology change produced by the 14 MeV neutron irradiation even at 293 K, shown in Fig. 5. Small pits of a few μm in diameter on the surface of $SrCe_{0.95}Yb_{0.05}O_{3-d}$ were smoothened by the irradiation to 1×10^{19}n/m^2, suggesting a long-distance migration of constituent ions at 293 K. In the case of electron irradiation at 293 K, formation of SrO fine needles on the $SrCe_{0.95}Yb_{0.05}O_{3-d}$ surface was observed, suggesting decomposition of $SrCe_{0.95}Yb_{0.05}O_{3-d}$ into SrO and $Ce_2O_{4-\delta}$ [23].

In the technologically important ceramic insulators such as alpha-alumina (Al_2O_3) and magnesia (MgO), the protonic conductivity is negligible, making a minimal contribution only above 1300 K. No clear evidence was obtained so far for the contribution of the protonic conductivity in the alpha-alumina was obtained during the JMTR irradiation. However, in a hydrogen-isotope rich environments with high dose rate irradiation, the protonic conductivity may play some role even in these ceramic insulators at relatively moderate temperatures.

3.3. Reduction of ions in the oxide during the irradiation

As described above, the decrease of the electrical conductivity by mechanisms 1 and 2 was observed

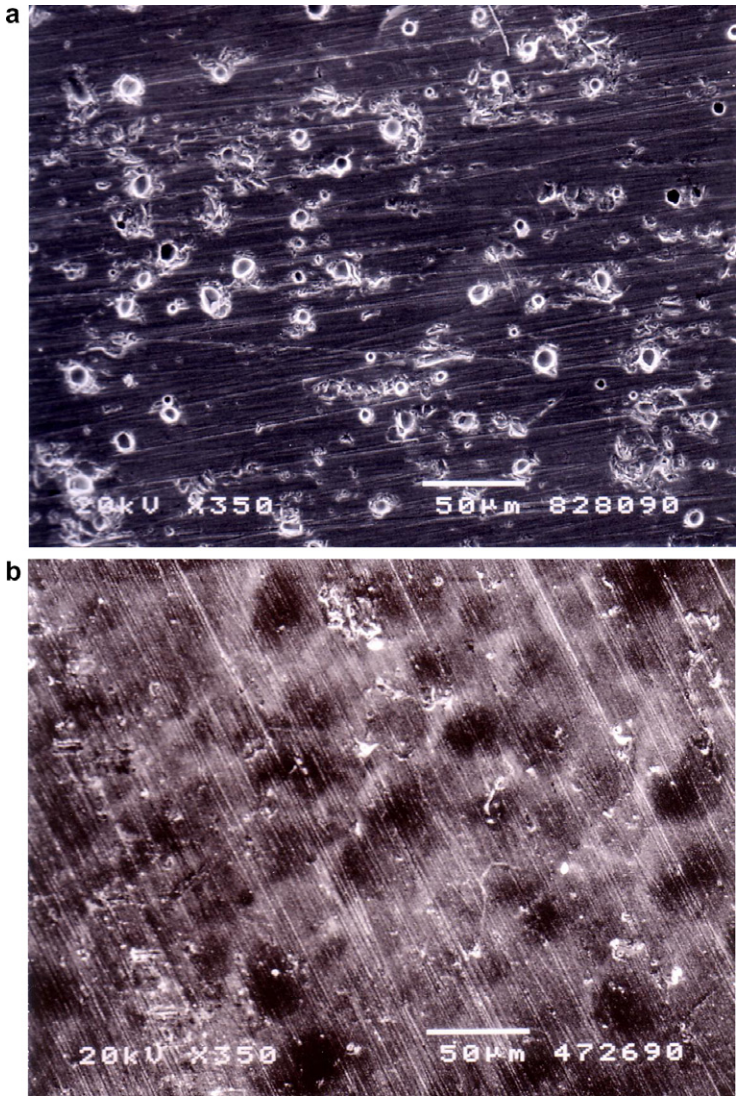

Fig. 5. Surface morphology change of $SrCe_{0.95}Yb_{0.05}O_{3-d}$ by 14 MeV neutron at room temperature. (a) Before irradiation, (b) after irradiation.

in the course of the irradiation. For mechanism 2, the decrease corresponds to the decrease of the proton concentration in the specimen as the supply of hydrogen was limited. Also, the radiation induced defects (increase of trap sites for protons) in the oxide will decrease the mobility of protons.

Assuming that mechanism 1 corresponds to the electronic or hole conductivity, the decrease of the electrical conductivity by mechanism 1 implies that some modification of electronic states was taking place in the oxide during the irradiation. Fig. 6 shows change in the optical transmission loss of $SrCe_{0.95}Yb_{0.05}O_{3-d}$ under 1.8 MeV electron irradiation at room temperature [24]. A large decrease in the optical transmission loss was observed in the wavelength range 500–800 nm, where a major optical absorption center in $SrCe_{0.95}Yb_{0.05}O_{3-d}$ is Ce^{4+}. Thus, the results are suggesting that the electron irradiation decreases the concentration of Ce^{4+}. The XPS confirmed change of the charge state of Ce in $SrCe_{0.95}Yb_{0.05}O_{3-d}$, from 4+ to 3+, namely reduction of Ce by the electron irradiation. The same results were obtained, for the 14 MeV neutron irradiation at room temperature. Before the irradiation, the spectrum corresponded to that for Ce^{4+}, which was converted into the spectrum for Ce^{3+} by the 1×10^{19} n/m^2 irradiation at room temperature [22].

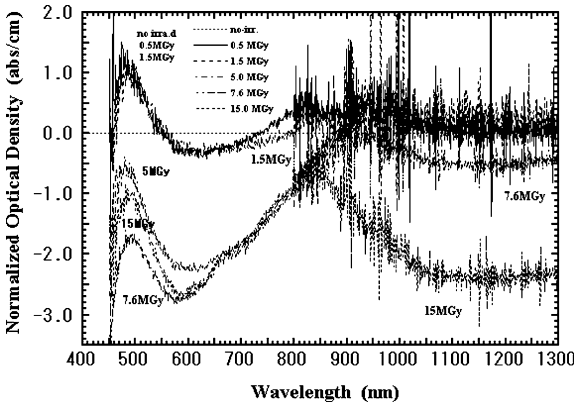

Fig. 6. Optical absorption of $SrCe_{0.95}Yb_{0.05}O_{3-d}$ under 1.8 MeV electron irradiation at room temperature.

The Ce^{4+} will provide an electronic conduction path and the reduction of Ce^{4+} to Ce^{3+} will decrease the number of electronic conduction path which corresponds to the decrease of the electrical conductivity by mechanism 1. In the case of hole conduction, the Ce^{3+} will work as trap sites and decrease the number of mobile holes.

The reduction of oxide ceramics by radiation effects at moderate temperatures is one of the important topics for fusion functional materials. In alpha-alumina, reduction of chromium, which is a typical optically sensitive impurity, from Cr^{3+} to Cr^{2+} through the interaction with an oxygen vacancy was reported [30,31]. With assistance by protons, the reduction of cations will take place even in the technological important ceramics, which may result in technological problems in fusion ceramics.

4. Conclusions

The behavior of electrical conductivity of perovskite-oxides was evaluated, under 1.8–2.0 MeV electrons, 14 MeV neutrons and fission reactor irradiations. Effects of hydrogen (protons) on the electrical conductivity were specially studied. All of the perovskite-oxides studied had relatively large base electrical conductivity and normal RIC by the excited electrons was marginal in the irradiation. The protonic conduction which was dominant above about 450 K was strongly enhanced by the irradiation. Also, the base electronic conduction was suppressed by the radiation induced reduction, in the case of $SrCe_{0.95}Yb_{0.05}O_{3-d}$, by reduction of Ce 4+ to Ce 3+. The presense of protons in oxides and the radiation effects will enhance the long-distance migration of ions and phase changes will take place at relatively low temperatures in these oxides. These may imply some technological problems for ceramics used in fusion systems.

Acknowledgements

The authors would like to express their sincere gratitude to their colleagues, Dr A. Morono in the CIEMAT, Professor S. Nagata and Dr K. Toh in the IMR, Tohoku University. The JMTR irradiation experiments were carried out under the close collaboration with Mr M. Narui of Oarai Branch of IMR, Tohoku University and the JMTR staffs in the JAEA. Finally, the authors would like to express their special thanks to Dr T. Nishitani of Naka, JAEA and his staffs in FNS, Tokai, JAEA.

References

[1] S. Yamamoto, Design Description Document, WBS 5.5 M, Radiation Effects, ITER-JWS Garching, Germany, 1999.
[2] S. Yamamoto, T. Shikama, V. Veryakov, E. Farnum, E. Hodgson, T. Nishitani, D. Orlinski, S. Zinkle, S. Kasai, P. Stott, K. Young, V. Zaveriaev, A. Costley, L. deCock, C. Walker, G. Janeschits, J. Nucl. Mater. 283–287 (2000) 60.
[3] A. Costley et al., Fus. Eng. Des. 55 (2001) 331.
[4] E.R. Hodgson et al., Irradiation effects in ceramics for heating and current drive and diagnostic systems, Report EUR-CIEMAT-95, 2003.
[5] T. Shikama, S.J. Zinkle, J. Nucl. Mater. 307–311 (2002) 1073.
[6] M. Decreton, T. Shikama, E. Hodgson, J. Nucl. Mater. 329–333 (2004) 125.
[7] T. Shikama, K. Yasuda, S. Yamamoto, C. Kinoshita, S.J. Zinkle, E.R. Hodgson, J. Nucl. Mater. 271&272 (1999) 560.
[8] E.R. Hodgson, J. Nucl. Mater. 179–181 (1991) 383.
[9] T. Shikama, S.J. Zinkle, K. Shiiyama, L.L. Snead, E.H. Farnum, J. Nucl. Mater. 258–263 (1998) 1867.
[10] T. Shikama, S.J. Zinkle, J. Nucl. Mater. 258–263 (1998) 1861.
[11] Benoit Brichard, A. Fernandez, H. Ooms, F. Berghmans, M. Decreton, A. Tomashuk, S. Klyamkin, M. Zabezhailov, I. Nikolin, V. Bogatyrjov, E. Hodgson, T. Kakuta, T. Shikama, T. Nishitani, A. Costley, G. Vayakis, J. Nucl. Mater. 329–333 (2004) 133.
[12] T. Shikama, T. Kakuta, N. Shamoto, M. Narui, T. Sagawa, Fus. Eng. Des. 51&52 (2000) 179.
[13] T. Shikama, Nucl. Instrum. and Meth. B 122 (1997) 650.
[14] T. Shikama, T. Nishitani, T. Kakuta, S. Yamamoto, S. Kasai, M. Narui, E. Hodgson, R. Reichle, B. Brichard, A. Krassilinikov, R. Snider, G. Vayakis, A. Costley, S. Nagata, B. Tsuchiya, K. Toh, Nucl. Fusion 43 (2003) 517.
[15] T. Nishitani, G. Vayakis, M. Yamauchi, T. Sugie, T. Kondoh, T. Shikama, E. Ishitsuka, H. Kawashima, J. Nucl. Mater. 329–333 (2004) 1461.

[16] G. Janeschitz, C. Walker, A. Costley, L. Dekock, K. Ebisawa, P. Edmonds, L. Johnson, S. Kasai, V. Mukhovatov, P. Stott, G. Vayakis, S. Yamamoto, K. Young, V. Zaveriaev, in: Proceedings of the 17th IAEA Conference on Fusion Energy, Yokohama, 19–24, October, 1998, ITERP1/15, IAEA, Vienna. <http://www.iaea.org/programmes/ripc/physics/>.
[17] T. Nishitani, T. Shikama, R. Reichle, E.R. Hodgson, E. Ishitsuka, S. Kasai, S. Yamamoto, Fus. Eng. Des. 63&64 (2002) 437.
[18] T. Shikama, T. Yamamoto, R. Snider, M. Fukao, T. Nishitani, K. Young, S. Kasai, M. Narui, J. Broesch, H. Matsuo, T. Sagawa, Fus. Eng. Des. 51&52 (2000) 171.
[19] G. Vayakis, T. Sugie, T. Kondoh, T. Nishitani, E. Ishitsuka, M. Yamauchi, H. Kawashima, T. Shikama, Rev. Sci. Instrum. 75 (2005) 4324.
[20] C. Walker, private communication, also in Ref. [1].
[21] B. Tsuchiya, S. Nagata, K. Saito K. Toh, T. Shikama, in: Proceedings of the Hydrogen Materials Science and Chemistry of Carbon Nanomaterials 2007, p. 133.
[22] B. Tsuchiya, S. Nagata, K. Toh, T. Shikama, M. Yamauchi, T. Nishitani, Fus. Sci. Technol. 47 (4) (2005) 891.
[23] B. Tsuchiya, A. Moroño, E.R. Hodgson, T. Yamamura, S. Nagata, K. Toh, T. Shikama, Phys. Stat. Sol. (C) 2 (1) (2005) 204.
[24] T. Shikama, Adv. Sci. Technol. 24 (1999) 463.
[25] T. Tanaka, T. Shikama, M. Narui, B. Tsuchiya, A. Suzuki, T. Muroga, Fus. Eng. Des. 75–79 (2005) 933.
[26] H. Iwahara, Solid State Ionics 77 (1995) 289.
[27] H. Uchida, H. Yoshikawa, T. Esaka, S. Ohtsu, H. Iwahara, Solid State Ionics 36 (1989) 89.
[28] B. Tsuchiya et al., J. Nucl. Mater, these Proceedings, doi:10.1016/j.jnucmat.2007.03.200.
[29] T. Arai, A. Kunimatsu, K. Takahiro, S. Nagata, S. Yamaguchi, Y. Akiyama, N. Sata, M. Ishigame, Solid State Ionics 121 (1999) 263.
[30] T.H. Maiman, Nature 187 (1960) 493.
[31] A.P. Vink, A. Meijerink, Spectrochim. Acta, Part A 54 (1998) 1755.